Daniel Flamm, Julian Hellstern, Andreas Heimes, Felix Zimmermann, Anbdolnaser Ghazagh, Jona Wohletz, Fabian Kimmich, Jonas Kleiner, and Christoph Tillkorn, "Multi-mJ ultrafast laser machining with flexible multi-spot patterns", Proc. SPIE 11994, High-Power Laser Materials Processing: Applications, Diagnostics, and Systems XI, 119940K (4 March 2022); https://doi.org/10.1117/12.2607612.

Multi-mJ ultrafast laser machining with flexible multi-spot patterns

Daniel Flamm,[a] Julian Hellstern,[b] Andreas Heimes,[a] Felix Zimmermann,[a] Abdolnaser Ghazagh,[a] Jona Wohletz,[a] Fabian Kimmich,[b] Jonas Kleiner,[a] and Christoph Tillkorn[b]

[a]TRUMPF Laser- und Systemtechnik GmbH, Johann-Maus-Str. 2, 71254 Ditzingen, Germany
[b]TRUMPF Laser GmbH, Aichhalder Str. 39, 78713 Schramberg, Germany

ABSTRACT

We demonstrate how high-energy ultrafast laser sources can be used to efficiently drive well-known low-energy micro-machining applications such as surface structuring of opaque and transparent materials. The presented optical concept employs micro-lens arrays, thus standard components, as central beam splitting elements to generate multiple focal spots for parallel processing. Here, a simple and robust opto-mechanical concept enables to control the number of foci ranging from a few ten up to a few hundred spots. Throughput scaling and complete use of the industry-grade ultrafast laser platform is discussed by means of selected micro-machining examples.

Keywords: Beam shaping, beam splitting, ultrafast optics, laser materials processing, structured light, micro-lens arrays

1. INTRODUCTION

The steady progress in increasing the energy and power performance of ultrafast laser systems[1–4] raises the question of how these destructive photonic states can be used for subtle machining in the micro- and nanoscale.[5] Spatio-temporal beam shaping represents the main enabler to cleverly distribute high energies onto large surfaces[6,7] or inside large volumes of workpieces.[5,8] We demonstrate a processing optics that consists of micro-lens arrays as central beam splitting elements to generate multiple focal spots for parallel micro-processing. The optics made of standard components is compatible for the use with conventional scan systems. A simple and robust opto-mechanical concept enables to control the number of foci ranging from a few ten up to a few hundred spots—a setup ideally suited for developing new material processing strategies.[7,9]
The efficacy of our beam shaping technique is demonstrated by means of selected processing examples which, using conventional focusing with single Gaussian spots, only require pulse energies in the single-digit or, at most, double-digit microjoule range. The micro-lens array-based processing head, however, enables the efficient usage of an industry-grade multi-millijoule and multi-hundred-watt laser platform even for the mentioned low-power applications simply by parallel processing. As examples, we present high-throughput surface structuring of transparent and opaque materials with picosecond pulses. During the processing we aim to exploit the complete power and energy performance of the industry-grade ultrafast laser platform.

2. BEAM SPLITTING USING ARRAYS OF MICRO LENSES

Microlens arrays (MLAs) are common to the beam shaping community as they represent of-the-shelf components especially useful for any kind of light homogenization.[7,10] It is also well known, that for a sufficiently high degree of coherence of the illuminating source, MLA-based homogenizer act as beam splitters generating almost ideal focus copies usually along Cartesian grids.[10–13] As this way of beam splitting is characterized by being particularly efficient without generating stray light or unwanted diffraction orders, this concept is excellently suited for high power and high energy laser materials processing.[11,14,15] The following sections will demonstrate that splitting into $\sim(100 \times 1)$ or $\sim(100 \times 100)$ focal spots becomes possible without major effort. Thus, parallel processing and throughput increase by several orders of magnitude are feasible.

Further author information:
E-Mail: daniel.flamm@trumpf.com.

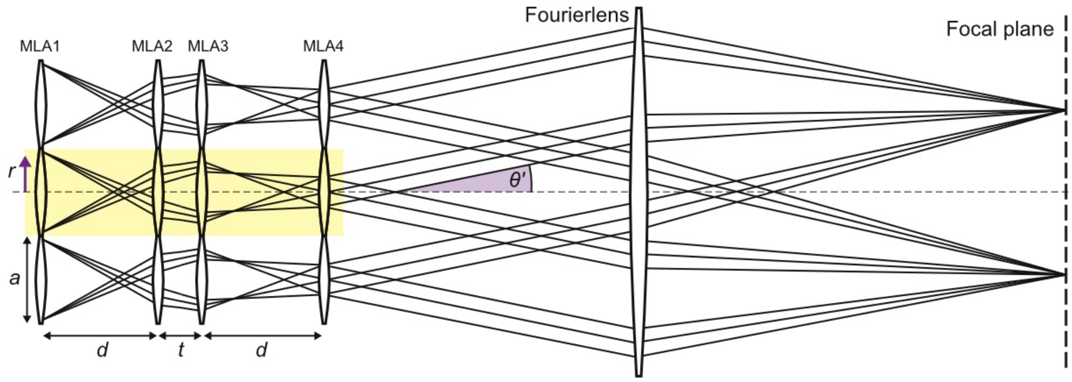

Figure 1. Scetch of the experimental setup with definition of the four MLA positions with distances d and t, respectively. The cell highlighted in yellow supports our discussion of considering the concept as a variable telescope in periodic replication. Every point r for every propagation angle θ is mapped into a well defined angular direction θ' by the set of MLAs in one unit cell.

Considering an optical system consisting of at least two cylindrical MLAs of equal pitch a with on-axis alignment, see Fig. 1, for a single unit cell, see yellow-colored lens system, an effective focal length f_{ML} can always be found.[9] Here, every point r for every propagation angle θ is mapped into a well defined angular direction θ'. For sufficient large beam diameters (or sufficient small unit cells), the diffractive impact of the MLAs to the radiation can be modeled using the grating equation $\lambda N \approx 2\theta' a$ (small angle approximation for total number of orders N, positive and negative diffraction orders). Additionally, taking into account that maximum diffraction angles θ' are determined by the effective focal length of the MLA set and corresponding pitch $2\theta' \approx a/f_{\mathrm{ML}}$, a fundamental relation is found linking MLA parameters with achievable diffraction orders N[9]

$$f_{\mathrm{ML}} = \frac{a^2}{\lambda N}. \tag{1}$$

The pitch a of the used MLAs is, thus, determining the maximum number of spots that can be generated by our beam splitting concept. For the special case of using the well-known imaging homogenizer setup,[10] thus, two identical MLAs with given f_{ML} and pitch a, Eq. (1) is valid if their distance d equals the focal length.

Coming back to the imaging properties of a single cell in the MLA setup, see again Fig. 1. Similar to well-known concepts of variable beam expanders, using more than two lenses with well defined distances, see distances d and t in the four-lens example of Fig. 1, the effective focal length $f_{\mathrm{ML}}\,(\theta')$ and, thus, the number of diffraction orders N [cf. Eq. (1)] can be precisely controlled. In the case of using four MLAs of pitch a and two focal lengths $f_{1,2}$ in a symmetric arrangement (MLA1: f_1, MLA2: f_2, MLA3: f_2, MLA4: f_1) with $f_2 = f_1/3$ the following relations for the distances d and t can be found[9]

$$d = \frac{f_{\mathrm{ML}} f_1 + f_{\mathrm{ML}} f_2 + f_1 f_2}{f_1 + f_{\mathrm{ML}}}, \tag{2}$$

$$t = f_2 \frac{f_1^2 f_2 - f_{\mathrm{ML}}^2 f_2 + 2 f_{\mathrm{ML}} f_1^2}{f_{\mathrm{ML}} f_1^2}. \tag{3}$$

Far-field operation for achieving spatially separated diffraction orders is realized by adding a Fourier-lens to our setup, see Fig. 1. The focusing unit with focal length f_{FL} is generating a number of N focus copies in the focal plane with spatial distance $\Delta x = \lambda f_{\mathrm{FL}}/a$.[16] As an example, we set up a beam splitting optics with four MLAs in the symmetric arrangement discussed above $a = 1.3\,\mathrm{mm}$, $f_1 = 28\,\mathrm{mm}$ and $f_2 = 7\,\mathrm{mm}$,* see Fig. 1. The results

*Note that with this choice of focal lengths, the important condition $f_1 = 3f_2$ only applies to a good approximation.[9] However, we will demonstrate with our experiments that uniform and flexible beam splitting will still be possible, cf. Fig. 3. The method presented here is therefore quite robust with respect to the optical specifications.

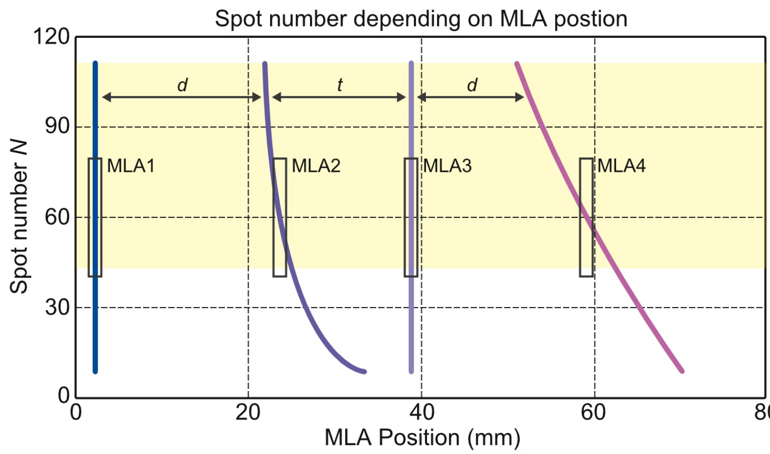

Figure 2. Absolute positions of the four cylindrical MLAs to generate a well-defined spot number N calculated via Eqs. (1) – (3). The yellow highlighted area where $N(d,t) \sim (40 \dots 100)$ shows an interesting special case where, in a very good approximation, the positions of MLA2 and MLA4 can be varied using a single axis stage as the respective curves follow almost linear dependencies with similar slopes.[9]

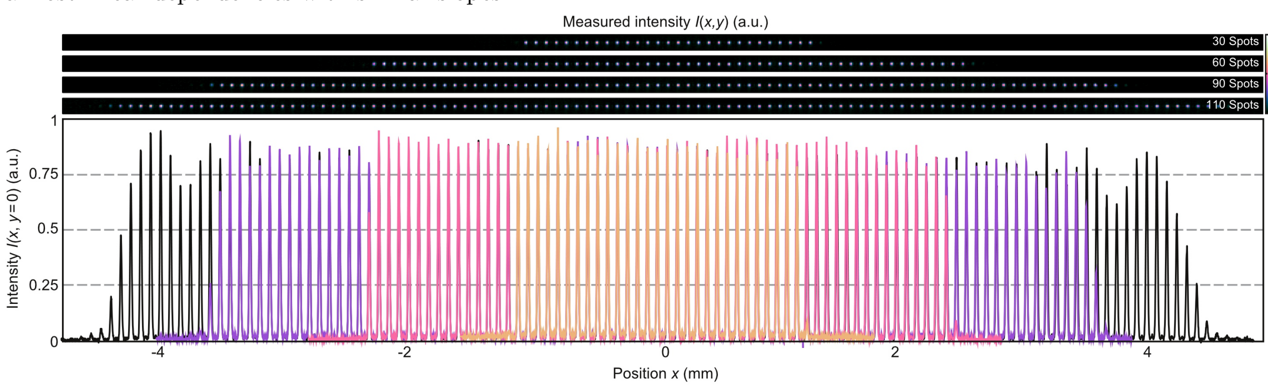

Figure 3. Characterization of the discrete line focus distribution with varying numbers of spots. Two-dimensional (top) and one-dimensional (bottom) intensity profiles generated by the MLA optics. The maximum number of spots shown in the black curve ($N \approx 110$) can be doubled using a polarization beam splitting concept $N' \approx 220$.[17]

for the distances d, t to flexibly split into $N \sim (10 \dots 100)$ spots is depicted in Fig. 2. Keeping the absolute positions of MLA1 and MLA3 constant while changing the positions of MLA2 and MLA4 within a few 10 mm only enables to vary the spot number by one order of magnitude. Please note that for the spot region highlighted in yellow $N \sim (40 \dots 100)$ the positions of MLA2 and MLA4 follow almost linear curves with similar slopes. Thus, in good approximation both lens arrays can be positioned using a single axis stage to achieve the desired spot number variation.[9]

Our solution for the positioning of the MLA set according to Eqs. (2) and (3), cf. Fig. 2, is mechanically realized using a combination of sleeve and carriage, which is common for zoom lens systems. To allow independent axial motion of MLA2 and MLA4 the movements are projected onto the cylindrical sleeve in a helical cam. The cam follower engages with the cam and transfers a rotation of the sleeve into an axial movement of MLA2 and MLA4, respectively. Using this concept, the required positioning accuracy of 200 μm and repeatability of 40 μm has been reached by this assembly.

For characterizing the beam splitting abilities of our optical concept a camera is placed in the focal plane to record the focus intensity distribution, cf. Fig. 1. A conventional f-θ-lens ($f_{\text{eff}} = 100\,\text{mm}$) acts as Fourier lens with MLA4 of the MLA-system located in its back focal plane. According the MLA positions stated in Fig. 2 we performed different measurements intended to split into a broad range of foci $N = (10 \dots 110)$. The resulting intensity measurements in a 2D $[I(x,y)]$ and 1D representation $[I(x, y=0)]$ are depicted in Fig. 3 where each single measurement is normalized to unit intensity. The successful beam splitting into a certain number of focus copies is clearly visible. Achieved relative uniformity errors depend on N and amount to $U_{\mathrm{err}} < 10\,\%$ for $N \leq 50$ and $U_{\mathrm{err}} > 20\,\%$ for $N > 50$. Overall efficiency of the MLA setup and the focusing unit was determined to be higher than 95 % in any of the investigated cases. An achieved angular spot separation of 0.9 mrad results in a maximum line length of about 8 mm at $f_{\mathrm{eff}} = 100\,\mathrm{mm}$ and $\lambda = 1030\,\mathrm{nm}$, see Fig. 3. With a raw beam diameter of 5 mm the focal line's fill factor is already at its maximum limit which can be recognized by the non-maximum interference contrast, see beating effects at the intensity minima between two spots. Thus, larger beam diameters are preferred for the used MLA pitch of $a = 1.3\,\mathrm{mm}$.

In order to further increase the focal line's spot density, a polarization beam splitter is used filling the intensity gaps with perpendicularly polarized spots (not shown in Fig. 3). The birefringent crystal is designed to imprint propagation angle differences between s- and p-polarized light which are transformed into a well-defined spatial offset by the Fourier lens.[17] As a result, the line length is kept constant and the spot number is doubled. Interference effects are suppressed due to the perpendicular polarization states.

The extension of our concept to the second spatial dimension and thus a significant increase in the possible throughput ($N \times N$) is given, for example, by using any kind of regular two-dimensional lens arrays[16,18] or simply by using crossed cylindrical MLAs.

In our model for the description of the beam splitting abilities of MLAs the diffractive nature was emphasized, see deduction of Eq. (1). Thus, by an MLA-based splitting of ultrashort laser pulses dispersion effects will be at hand. An estimation via the grating equation and the spectral properties of ultrashort band-limited pulses shows that in our setup the diffraction angles for the respective spectral components have a significant difference only at less than 300 fs. For the picosecond pulses used in our experiments (Sec. 3), we did not see any influences, such as broadened diffraction orders or intensity losses, even for $N \rightarrow \max$, see Fig. 3.

Similar to conventional beam splitting concepts based on, e.g., diffractive optics,[19] the MLA optics is generating almost identical focus copies (in terms of intensities).[5,8,19] This means that additional beam shaping elements, such as flat-top field mappers or axicons, can also be applied here. The beam-split foci will then all exhibit the desired shape, for example flat-tops or ring-like distributions.[5,20]

At this section's end we would like to point out that, although we are using a highly dynamic axis system for workpiece movement (Sec. 3), the flexible MLA-based beam splitting concept is compatible with conventional scanning systems, too. The available scanning field will be determined by the focusing quality of the scanning objective. The decisive factor here is the existing distortion,[21] which cannot be compensated by the scan path in the case of a line focus.

3. HIGH-ENERGY SURFACE STRUCTURING

The flexible beam splitting concept introduced in the previous section is applied to multi-mJ ultrashort laser pulses emerging from a TruMicro Series 6000 laser.[22] This industrial laser source provides picosecond pulses with average powers of 200 W. Operating at 25 kHz a maximum pulse energy of 8 mJ (equally distributed into four subpulses) can be extracted. The following two sections demonstrate the beneficial use of the beam splitting optics to efficiently structure large surfaces of transparent substrates (Sec. 3.1) and metals (Sec. 3.2), respectively. In both cases, single spot modifications merely require pulse energies in the single digit microjoule level. Only the parallel processing enables to exploit the complete energy performance of the laser system and to develop efficient material processing strategies generating high throughputs.[5,6,23]

With the machining results presented in the following, we do not claim to have found optimum processing parameters or results. These are relevant but freely chosen examples demonstrating throughput scaling with high-energy lasers by applying parallel processing from flexible multi-spot profiles.

3.1 Ultrafast laser surface texturing of transparent materials

Surface structuring is a well-established laser micro-processing discipline providing novel surface properties and functionalization for familiar materials.[24–26] Considering transparent materials, such properties may be connected to enhanced abilities regarding liquid repulsion, haptical impression, self cleaning, etc. One procedure that is frequently aimed is the creation of tiny surface sinks called dimples. Depending on the exact application,

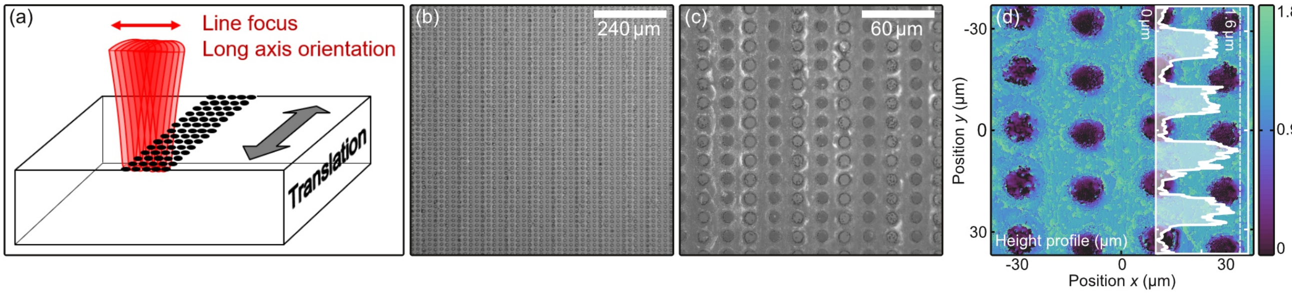

Figure 4. Ultrafast laser surface processing of transparent materials. Schematic of the focusing concept with long axis orientation perpendicular to the feed direction (a). Microscope image with different details of the processed substrates (b), (c). Height profile measurement with two- and one-dimensional plots of the processed surface (d).

these surface dimples can be a few micrometers wide and as shallow as a few hundred nanometers.[27] As a single-pulse process, it is mainly the dimple dimension that determines the required pulse energy. For the task at hand 10 µm-diameter dimples with a fill factor of about 50 % should be generated. Conveniently, Gaussian-like (single-mode) spots of 15 µm diameter can provide the desired dimple dimensions. In a preliminary experiment with single Gaussian spots and single pulse trains (four subpulses with 20 ns delay)[28] we determined the required burst energy to generate single dimples to $E_{\mathrm{pulse}} = 36\,\mu\mathrm{J}$ at 3 ps.

Using the optical setup described in Sec. 2 (with $f_{\mathrm{FL}} = 100\,\mathrm{mm}$) and a raw beam diameter of $d_0 = 9\,\mathrm{mm}$ we achieved focal spots of about 15 µm diameter. For parallel processing, the MLA optics was set to yield a spot number of $N = 90$ which was doubled by the polarization beam splitter to $N' = 180$ and illuminated with ultrashort laser pulses of 6.5 mJ burst energy. During processing, the line was oriented as depicted in the schematic of Fig. 4 (a) where the line focus' long axis was aligned perpendicular to the translation of the workpiece. To achieve the aimed fill factor, substrate translation parallel to this long axis is possible to fill the modification gaps by multiple slightly shifted passes. With a repetition rate of 25 kHz processing an area of $(100 \times 100)\,\mathrm{mm}^2$ in less than 15 s is achieved. Details of the processed borosilicate wafer can be seen in the microscope images depicted in Fig. 4 (b) and (c). A laser scanning microscope image confirms the successful dimple structuring with depths of about 1 µm, see height profile measurement in Fig. 4 (d).

3.2 Ultrafast laser line engraving of metals

For changing the tribological behavior of opaque materials such as metals, ultrafast lasers represent a state-of-the-art technology for, e.g., reducing friction coefficients or improving wears resistances.[25,29,30] In the present task, microlines are to be engraved in steel exceeding 20 µm width and 10 µm depth with $\sim$ m/s feed rates (other groove aspect ratios feasible[6]). Efficient picosecond ablation/engraving of metals with Gaussian-like spots is typically achieved at $\sim 1\,\mathrm{J/cm}^2$.[6,31] Considering a single spot ablation on the area of a 20 µm-diameter circle, pulse energies in the order of a single digit µJ would be required. We, therefore, set our beam splitting optics to generate the maximum spot number of $N' = 220$ and exploit a pulse energy of 0.5 mJ from the source. Using a Gaussian raw-beam diameter of 4.5 mm and the same focusing unit from previous section, cf. 3.1 ($f_{\mathrm{FL}} = 100\,\mathrm{mm}$) Gaussian spots of $\sim 30\,\mu\mathrm{m}$ diameter are generated and focused onto the workpiece, cf. Fig. 1. For the line engraving experiments, the line focus' long axis was oriented parallel to the feed rate, see Fig. 5 (a). A multitude of parallel running grooves of 80 µm pitch can be seen in the microscope images depicted in Fig. 5 (b) and (c). Due to the beam splitting, we perform 220 passes in a single process step and achieve the desired groove geometry free of significant burr, see height profile measurement in Fig. 5 (d). Operating with a maximum repetition rate of 200 kHz and spatial pulse distances of 15 µm enables feed rates of about $\sim 3\,\mathrm{m/s}$.

4. CONCLUSION

We presented a simple optomechanical concept to flexibly split ultrafast laser radiation from 10 to more than 200 spots. The refractive beam splitter made of standard micro-lens arrays (MLAs) enables to efficiently perform well-known low pulse energy micro-machining processes with high-energy, multi-mJ, industrial sources such as the TruMicro Series 6000 laser.[22] High efficiency is achieved through hundredfold beam splitting and associated

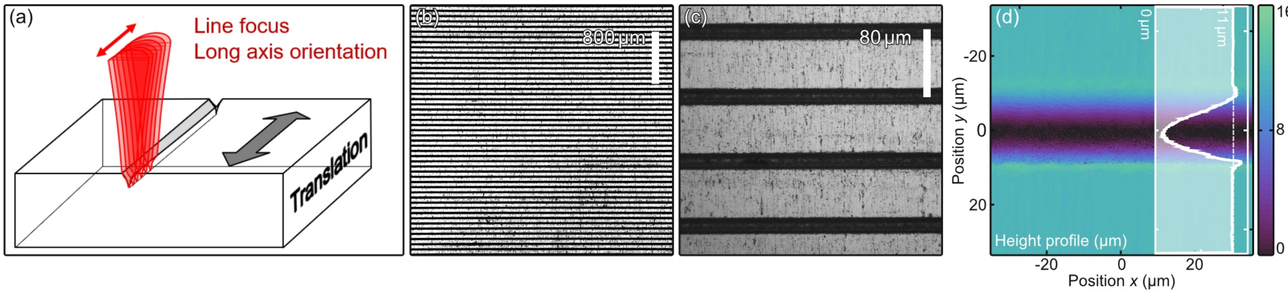

Figure 5. Ultrafast laser surface engraving of metals. Schematic of the focusing concept with long axis orientation parallel to the feed direction (a). Microscope image with different details of the processed samples (b), (c). Height profile measurement with two- and one-dimensional plots of a single engraved line (d).

throughput scaling. The flexibility in the number of spots provided by the MLA optics is beneficial for developing completely new application processes, and represents a clear advantage in comparison to standard stationary beam splitting concepts that are based on, e.g., diffractive optics. Throughput scaling with high yields relevant for industrial processes was demonstrated by means of selected texturing experiments on the surface of opaque and transparent materials, respectively. The MLA-based beam splitter is compatible with optical scanning systems and can be combined with addional beam shaping elements, such as, e.g., flat-top field mappers or axicons.

REFERENCES

1. C. J. Saraceno, D. Sutter, T. Metzger, and M. A. Ahmed, "The amazing progress of high-power ultrafast thin-disk lasers," *Journal of the European Optical Society-Rapid Publications* **15**(1), pp. 1–7, 2019.
2. D. H. Sutter, T. Dietz, D. Bauer, R. Scelle, A. Budnicki, A. Killi, M. Jenne, J. Kleiner, D. Flamm, M. Sailer, *et al.*, "High power and high energy ultrafast disk lasers for industrial applications," in *CLEO: Applications and Technology*, pp. JM3E–2, Optical Society of America, 2019.
3. M. Müller, C. Aleshire, A. Klenke, E. Haddad, F. Légaré, A. Tünnermann, and J. Limpert, "10.4 kW coherently combined ultrafast fiber laser," *Optics Letters* **45**(11), pp. 3083–3086, 2020.
4. T. G. Mans, M. Blecher, A. Hage, C. Paradis, M. Swantusch, J. Dolkemeyer, and C. Schnitzler, "High average power 10GW laser sources," in *Solid State Lasers XXX: Technology and Devices*, **11664**, p. 116640O, International Society for Optics and Photonics, 2021.
5. D. Flamm, D. G. Grossmann, M. Sailer, M. Kaiser, F. Zimmermann, K. Chen, M. Jenne, J. Kleiner, J. Hellstern, C. Tillkorn, *et al.*, "Structured light for ultrafast laser micro-and nanoprocessing," *Optical Engineering* **60**(2), p. 025105, 2021.
6. M. Kumkar, M. Kaiser, J. Kleiner, D. Flamm, D. Grossmann, K. Bergner, F. Zimmermann, and S. Nolte, "Throughput scaling by spatial beam shaping and dynamic focusing," in *Laser Applications in Microelectronic and Optoelectronic Manufacturing (LAMOM) XXII*, **10091**, p. 100910G, International Society for Optics and Photonics, 2017.
7. C. Tillkorn, A. Heimes, D. Flamm, S. Dorer, T. Beck, J. Hellstern, F. Marschall, and C. Lingel, "Anamorphic beam shaping for efficient laser homogenization: methods and high power applications," in *Laser Resonators, Microresonators, and Beam Control XX*, **10518**, p. 105181I, International Society for Optics and Photonics, 2018.
8. D. Flamm, M. Kaiser, M. Feil, M. Kahmann, M. Lang, J. Kleiner, and T. Hesse, "Protecting the edge: Ultrafast laser modified C-shaped glass edges," *Journal of Laser Applications* **34**(1), p. 012014, 2022.
9. C. Tillkorn, D. Flamm, J. Hellstern, A. Heimes, L.-W. Chang, and M. Prossotowicz, "Optical assembly for variably generating a multi-focus profile," June 3 2021. US Patent App. 17/149,769.
10. M. Zimmermann, N. Lindlein, R. Voelkel, and K. J. Weible, "Microlens laser beam homogenizer: from theory to application," in *Laser Beam Shaping VIII*, **6663**, p. 666302, International Society for Optics and Photonics, 2007.

11. S. Matsuo, S. Juodkazis, and H. Misawa, "Femtosecond laser microfabrication of periodic structures using a microlens array," *Applied Physics A* **80**(4), pp. 683–685, 2005.
12. M. Prossotowicz, A. Heimes, D. Flamm, F. Jansen, H.-J. Otto, A. Budnicki, A. Killi, and U. Morgner, "Coherent beam combining with micro-lens arrays," *Optics Letters* **45**(24), pp. 6728–6731, 2020.
13. M. Prossotowicz, D. Flamm, A. Heimes, F. Jansen, H.-J. Otto, A. Budnicki, A. Killi, and U. Morgner, "Dynamic focus shaping with mixed-aperture coherent beam combining," *Optics Letters* **46**(7), pp. 1660–1663, 2021.
14. A. Büttner and U. D. Zeitner, "Wave optical analysis of light-emitting diode beam shaping using microlens arrays," *Optical Engineering* **41**(10), pp. 2393–2401, 2002.
15. H. Muenz, A. Herkommer, and R. Egger, "Optical illumination system for creating a line beam," May 26 2009. US Patent 7,538,948.
16. M. Prossotowicz, A. Heimes, D. Flamm, F. Jansen, H.-J. Otto, A. Budnicki, U. Morgner, and A. Killi, "Dynamic coherent beam combining based on a setup of microlens arrays," in *Laser Resonators, Microresonators, and Beam Control XXII*, **11266**, p. 1126612, International Society for Optics and Photonics, 2020.
17. D. Flamm and M. Kumkar, "Verfahren zur Laserbearbeitung eines Werkstücks, Bearbeitungsoptik und Laserbearbeitungsvorrichtung," Nov. 14 2019. German Patent App. 10 2019 217 577.
18. M. Cumme and A. Deparnay, "From regular periodic micro-lens arrays to randomized continuous phase profiles," *Advanced Optical Technologies* **4**(1), pp. 47–61, 2015.
19. F. Wyrowski, H. van Esdonk, R. J. Zuidema, S. Wadmann, and G. J. Notenboom, "Use of diffractive optics in material processing," in *Diffractive and Holographic Optics Technology*, **2152**, pp. 139–144, International Society for Optics and Photonics, 1994.
20. F. M. Dickey, S. C. Holswade, *et al.*, *Laser beam shaping*, Marcel Dekker New York, 2000.
21. L. Büsing, *Optische Systeme für die hochpräzise, scannerbasierte Multistrahlbearbeitung mit ultrakurzen Laserpulsen*. PhD thesis, RWTH Aachen, 2016.
22. F. Jansen, A. Budnicki, and D. Sutter, "Pulsed lasers for industrial applications: Fiber, slab and thin-disk: Ultrafast laser technology for every application," *Laser Technik Journal* **15**(2), pp. 46–49, 2018.
23. M. Kumkar, M. Kaiser, J. Kleiner, D. Grossmann, D. Flamm, K. Bergner, and S. Nolte, "Ultrafast laser processing of transparent materials supported by in-situ diagnostics," in *Laser Applications in Microelectronic and Optoelectronic Manufacturing (LAMOM) XXI*, **9735**, p. 97350P, International Society for Optics and Photonics, 2016.
24. A. Žemaitis, M. Gaidys, M. Brikas, P. Gečys, G. Račiukaitis, and M. Gedvilas, "Advanced laser scanning for highly-efficient ablation and ultrafast surface structuring: experiment and model," *Scientific Reports* **8**(1), pp. 1–14, 2018.
25. D. N. Basha, G. Padmanabham, and R. Bathe, "Tribological behavior of surface textured gray cast iron at different texture density by ultrafast laser," *Materials Performance and Characterization* **8**(6), pp. 1147–1158, 2019.
26. J. Houzet, N. Faure, M. Larochette, A.-C. Brulez, S. Benayoun, and C. Mauclair, "Ultrafast laser spatial beam shaping based on Zernike polynomials for surface processing," *Optics Express* **24**(6), pp. 6542–6552, 2016.
27. F. Liang, R. Vallée, and S. L. Chin, "Physical evolution of nanograting inscription on the surface of fused silica," *Optical Materials Express* **2**(7), pp. 900–906, 2012.
28. P. R. Herman, R. Marjoribanks, and A. Oettl, "Burst-ultrafast laser machining method," Apr. 22 2003. US Patent 6,552,301.
29. K. Ahmmed, C. Grambow, and A.-M. Kietzig, "Fabrication of micro/nano structures on metals by femtosecond laser micromachining," *Micromachines* **5**(4), pp. 1219–1253, 2014.
30. F. Fraggelakis, G. Mincuzzi, J. Lopez, I. Manek-Hönninger, and R. Kling, "Texturing metal surface with MHz ultra-short laser pulses," *Optics Express* **25**(15), pp. 18131–18139, 2017.
31. B. N. Chichkov, C. Momma, S. Nolte, F. Von Alvensleben, and A. Tünnermann, "Femtosecond, picosecond and nanosecond laser ablation of solids," *Applied Physics A* **63**(2), pp. 109–115, 1996.